UDC 616.441-08:546.137 Original scientific paper

## DIAZEPAM'S EFFECTS ON HISTOLOGICAL CHANGES IN CEREBELLUM, CEREBRUM, PANCREAS AND THYROID GLAND TISSUES IN RATS

Jovana Grahovac<sup>1</sup>, Milenka Ivanović<sup>1</sup>, Radoslav Dekić<sup>†1</sup>, Maja Šibarević<sup>1</sup>, Smiljana Paraš<sup>1\*</sup>

<sup>1</sup>University of Banja Luka, Faculty of Natural Sciences and Mathematics, Mladena Stojanovića 2, 78000 Banja Luka, Republic of Srpska, Bosnia and Herzegovina \*Correspondent author: smiljana.paras@pmf.unibl.org

#### **Abstract**

Diazepam is a drug that is widely used today for the medical treatment of humans. It can serve as a primary medication for neurological disorders or as an adjunct therapy for symptomatic treatment. Diazepam induces a relaxing effect as a result of its sedative action on the central nervous system. Through its direct influence on the nervous system, diazepam disrupts the proper functioning of all organs in the human body. The aim of this study is to expand previous research on the effects of diazepam on histological parameters of the cerebrum, cerebellum, pancreas, and thyroid gland in rats. Experimental design included two groups of experimental animals, one of which was treated with diazepam while the other was not. To achieve the study's objectives, Mallory-Azan and immuno-histochemical staining methods (BLX-CX and Survivin) were used on rat organ tissues. Cytometric analysis detected cells undergoing apoptosis, and stereological parameter measurements were performed using a stereological universal test system based on Cavalieri's principle. Results of the histological and stereological parameter analysis indicate changes in the cytoarchitecture of the cerebrum, cerebellum, pancreas, and thyroid gland tissues in rats treated with diazepam compared to control group. Alterations in the histological parameters of the analyzed rat organ tissues directly demonstrate that diazepam affects their proper structure and function. This study provides a foundation for further detailed scientific research aimed at elucidating the existing effects of diazepam on all organs in the rat organism.

**Key words**: diazepam, cerebrum, cerebellum, pancreas, thyroid gland

## INTRODUCTION

Diazepam and similar drugs are increasingly used in modern medicine to alleviate stress symptoms in contemporary individuals. Health issues caused by stress lead people to self-medicate more frequently with various sedatives. The most common symptoms of stress include restlessness, tension, irritability, anxiety, anger, fear, insomnia, and other related symptoms (Sevastre-Berghian *et al.*, 2017). Benzodiazepines, a class of organic compounds, were introduced in the 1950s as sedatives for human use. Drugs from the benzodiazepine class are still widely used today for calming, pain relief, as anxiolytics, muscle relaxants,

anticonvulsants, hypnotics, and for inducing short-term amnesia (Olfson *et al.*, 2015). Diazepam is the name of a drug also known under several generic names, such as Valium®, Apaurin®, and Bensedin® (Amorim *et al.*, 2008). The sedative effect of benzodiazepines occurs due to their calming action on the central nervous system (CNS), where they selectively act on polysynaptic pathways by stimulating the inhibitory action of the neurotransmitter GABA (Aleksandrov *et al.*, 1999). Benzodiazepines act as depressants on the CNS by facilitating the binding of gamma-aminobutyric acid (GABA) to various GABA receptors throughout the CNS (Ashton, 2005). Increased GABA receptor activity reduces neural activity at specific sites in the brain (Mimica *et al.*, 2002; Malcolm, 2003).

Literature data indicate not only the positive but also the harmful effects of diazepam on hematological and biochemical parameters as well as on the histological parameters of organs (Honeychurch et al., 2014; Owen et al., 1970). Long-term use of diazepam may contribute to the development of diabetes, Alzheimer's disease, cardiopathy, liver toxicity, impaired kidney metabolism, or dysfunction of endocrine glands in humans (Pomares et al., 2017). Although beneficial and with a broad spectrum of action, these drugs have become one of the leading public health concerns due to their irrational use. Both directly and through its effects on the CNS, diazepam disrupts the proper functioning of all organs in the body (Anber et al., 2018). The use of diazepam can lead to capillary blockage due to impaired metabolite turnover. Additionally, it affects pancreatic degeneration, the formation of microvesicles, and necrosis in pancreatic tissue, resulting in pancreatic toxicity (Ilesanmi et al., 2020). Diazepam causes irreversible histological damage to the thyroid gland in rats, leading to its impaired function (Setiawan et al., 2016). In the tissues of the cerebellum and cerebrum of rats, diazepam accumulates after prolonged oral administration. Additionally, long-term use of diazepam leads to cellular damage and deterioration of the neuronal architecture in the cerebellum and cerebrum of rats (Eman et al., 2021). The aim of this study is to monitor the effects of diazepam (Bensedin®) on the histological parameters of the cerebellum, cerebrum, pancreas, and thyroid gland in Wistar rats.

## MATERIALS AND METHODS

The experiment was conducted at the Faculty of Natural Sciences and Mathematics, University of Banja Luka. The research lasted 14 days, and the experiment involved Wistar strain rats, two months old, with a total of 10 male individuals randomly divided into two experimental groups of five each. All animal procedures were in compliance with Directive 2010/63/EU on the protection of animals used for experimental and other scientific purposes and were approved by the Ethical Committee on Animal Experiments at the Faculty of Natural Sciences and Mathematics, University of Banja Luka, No. 01-9-192.2/20, Bosnia and Herzegovina. The first group of five individuals represented the control group, which received water at the same time as the treated group received diazepam. The second group of five individuals was the treated group, which was administered diazepam (Bensedin®, Galenika a.d., Belgrade, Republic of Serbia). The Bensedin solution and water were administered via oral intubation using a 5 ml pipette, final volume of solution approximately 2 ml. Rats in the treated group received a diazepam solution at a dose of 0.2 mg/kg. All animals from both experimental groups and control groups were kept under controlled

lighting conditions (12 h light - 12 h dark), at a temperature of 24°C, and controlled humidity. All rats in our experiment were fed standardized pelleted food for experimental animals and had access to water *ad libitum*.

Rats were decapitated in ether anesthesia after two weeks of treatment. Four organs of all rats were taken for analysis: cerebellum, cerebrum, pancreas and thyroid gland. The rats' organs immersed in Bouin's solution for 24h; for better fixative penetration, tissue was further cut into smaller pieces and then immersed into fresh Bouin's solution. Samples of tissues of all organs were embedded in paraffin, and were cut in a frontal plane on a Leica rotary Microtome RM 2165 (Leica Mycrosystems, Wetzlar, Germany), in 5 µm thick serial sections. All samples were stained with hematoxylin-eosin (H&E) and Mallory-Azan (all stains by Merck KGaA, Darmstadt, Germany). Cytometric (stereological and morphometric) analysis detected cells in apoptosis, using immunohistochemical staining methods BLX-CX and Survivin. The sections were then incubated with primary rabbit antibodies to glucagon (1:75; DakoCitomation) at 4 ° C overnight in a humid atmosphere. Negative control staining slides were incubated in the absence of primary antibody. The qualitative histology analysis of the tissue slides was performed while using the light microscope a Leica DM8000 microscope with a MEGA VIEW camera and software system for digital image transfer. Measurements were made using a stereo-universal test system according to Cavalier's principle, with using 16.0 point-counting system (MBF software system Application Suite 3.0.0, MBF Bioscience, Williston, VT, USA), with P2 spacing grid at the maximum 400X magnification (Nestorović et al., 2016). The volume of analyzed tissue was evaluated as the product of the number of counted frames ( $\Sigma$ Pi), the space of counted frame (a=25002), and the height factor (h) in the histological section, as presented in the following formula (Paraš et al., 2019):

$$Nv = \frac{Q}{Vo} = \frac{Q}{\sum_{i=1}^{n} Pi \times a \times h} \text{ (mm}^{-3})$$

Stereological analysis parameters included tissue or cell volume density, cell count, numerical cell density, cell surface area, nuclear surface area of the cells forming the analyzed tissue, nucleocytoplasmic ratio (NCR), and mitotic and apoptotic cell indices. Statistical data analysis was performed using OriginPro, a Microsoft Windows program, version 10.5.91.46291/2018, USA. Statistical differences between the control and treated groups were determined using the t-test and Dunnett's test.

## **RESULTS**

Histological analysis of cerebrum, cerebellum, pancreas and thyroid gland tissues of rats treated with Bensedin shows changes in architecture and vascularization of their cellular elements compared to the appropriate control group. Stereological analysis of treated and control rats detects changes in mean values of stereological parameters (Tables 1-4).

**Table 1.** Stereological parameters of the cerebrum tissue of the control and experimental group of rats, value are shown as mean±SD (\*p<0.05; t-test)

Parameters	Control	Bensedin
Volume density of granular neurons (mm <sup>0</sup> )	0.275±0.041	0.296±0.045
Volume density of pyramidal neurons (mm <sup>0</sup> )	0.296±0.035	0.268±0.033
Volume density of neuroglia (mm <sup>0</sup> )	0.219±0.022	0.195±0.021
Volume density of capillary sinusoids (mm <sup>0</sup> )	0.201±0.017	0.245±0.020
Number of granular neurons	142435.4±15902.5	152134.7±18911.3
Numerical density of granular neurons (mm <sup>-3</sup> )	24142.3±1102.7	21740.5±1245.5
Surface area of granular neurons (µm²)	69.5± 9.2	65.2±8.1
Surface area of granular neurons' nuclei (µm²)	29.8±7.9	28.4±6.6
NCR of granular neurons	0.369±0.041	0.372±0.044
Number of pyramidal neurons	122174.1±23471.3	77649.3±10201.8*
Numerical density of pyramidal neurons (mm <sup>-3</sup> )	11167.6±8724.9	6045.7±5352.5*
Surface area of pyramidal neurons (μm²)	188.2±24.7	125.4±21.4*
Surface area of pyramidal neurons' nuclei (µm²)	92.7±10.5	64.9±10.8
NCR of pyramidal neurons	0.333±0.029	0.305±0.031
Number of neuroglia	103025.2±18541.4	91832.7±15322.1
Numerical density of neuroglia (mm <sup>-3</sup> )	10025.6±1503.2	9112.4±1424.3
Surface area of neuroglia (µm²)	47.5±9.6	45.5±9.2
Surface area of neuroglia' nuclei (µm²)	29.4±7.6	28.8±7.2
NCR of neuroglia	0.452±0.056	0.487±0.059
Apoptotic index of neuroglia	0.00±0.00	1.06±0.099*
Number of capillary endothelial cells	170632.1±85325.6	199434.8±95223.1
Numerical density of capillary endothelial cells (μm²)	16791.4±4872.4	17902.3±7003.6
Surface area of capillary endothelial cells (µm²)	98.9±11.2	101.5±11.8

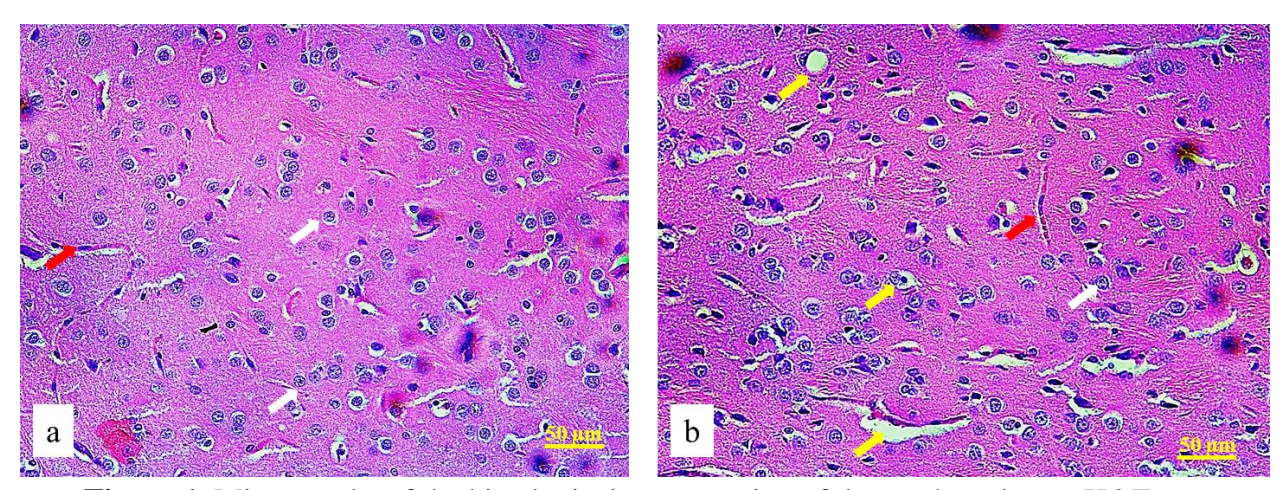


**Figure 1.** Micrographs of the histological cross-section of the rats´ cerebrum, H&E, magnification 100X. Increased volume density and number of granular neurons (white arrows), microcavities (yellow arrows) and increased capillary sinusoids (red arrows); control (a) and treated group (b)

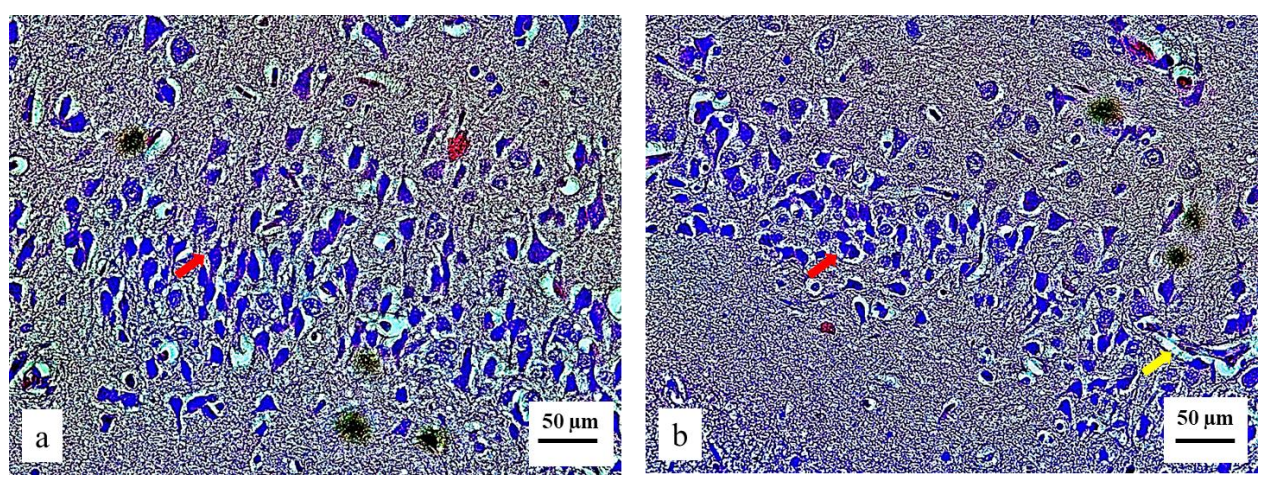


**Figure 2.** Micrographs of the histological cross-section of the rats' cerebrum, Cresyl-violet, magnification 100X. Pyramidal neurons (red arrows) and blood vessels (yellow arrows); control (a) and tissue with treatment to Bensedin (b)

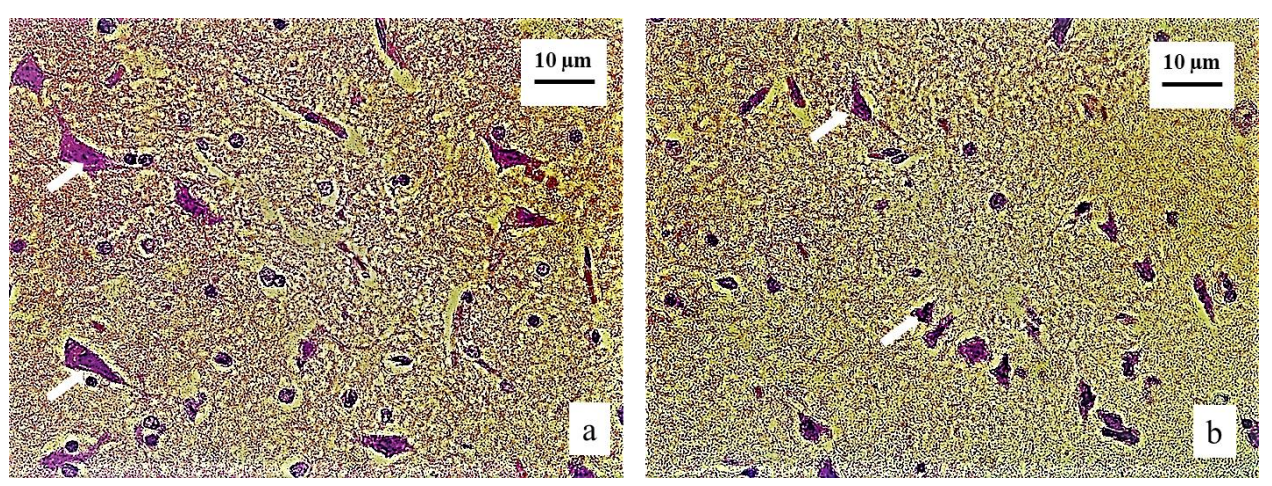


**Figure 3.** Micrographs of the histological cross-section of the rats´ cerebrum, Mallory-Azan, magnification 200X. Pyramidal neurons (white arrows) and neuroglia; control (a) and tissue with treatment to Bensedin (b)

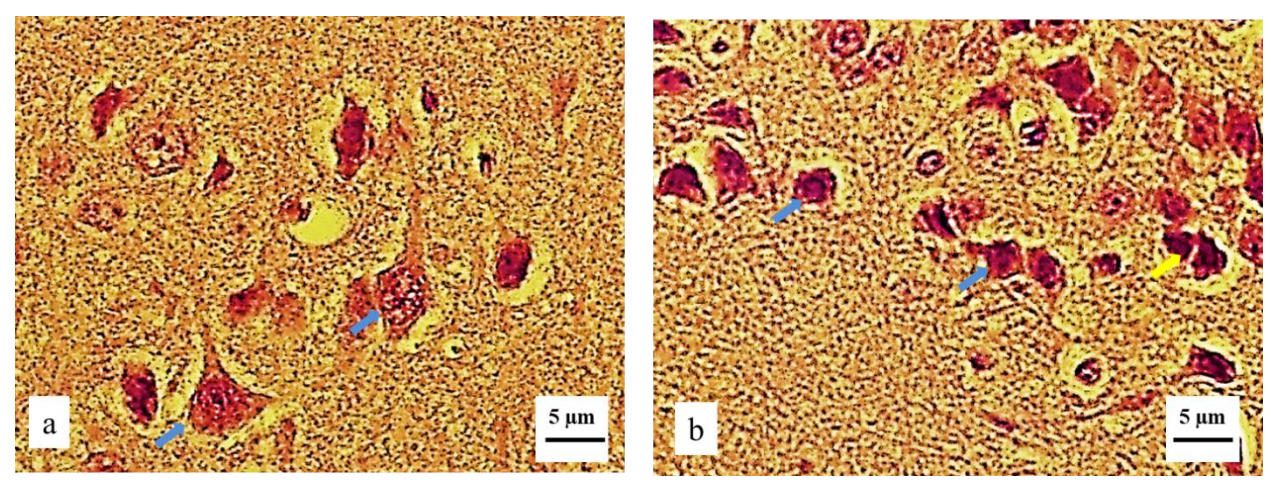


**Figure 4.** Micrographs of the histological cross-section of the rats' cerebrum, Survivin, magnification 400X. Pyramidal neurons (blue arrows) and apoptotic neuroglia (yellow arrows); control (a) and tissue with to Bensedin (b)

In addition to an increase in sinusoidal capillaries in cerebrum of rats treated with Bensedin, microcavities (Figure 1) also appeared, which are absent in cerebrum tissue of the control rats. Number and numerical density of granular cells and neuroglia statistically insignificantly decrease, while sinusoidal capillaries increase in the animals treated with Bensedin. On the other hand, number (p=0.031), numerical density (p=0.034), and surface area of pyramidal neurons (p=0.042) in cerebrum statistically significantly decrease in Bensedin treated rats compared to the controls (Figures 2 and 3). Cerebrum tissues of the Bensedin treated rats showed a markedly altered shape of pyramidal neurons, indicating a loss of neurites and intercellular communication. Neurons in mitosis were not detected in tissue sections from the cerebrum of rats in either experimental group, but neuroglia in apoptosis were observed using immunohistochemical staining (Figure 4).

**Table 2.** Stereological parameters of the cerebellum tissue of the control and experimental group of rats, value are shown as mean±SD (\*p<0.05; t-test)

Parameters	Control	Bensedin
Volume density of stratum moleculare (mm <sup>0</sup> )	0.432±0.079	0.425±0.0.087
Volume density of Purkinje cells (mm <sup>0</sup> )	0.109±0.018	0.093±0.021
Volume density of stratum granulosum (mm <sup>0</sup> )	0.332±0.022	0.341±0.025
Volume density of capillary sinusoids (mm <sup>0</sup> )	0.112±0.014	0.114±0.016
Number of neurons in stratum moleculare	102691.5±12654.7	93027.2±8023.4
Numerical density of neurons in stratum moleculare (mm <sup>-3</sup> )	8284.6±756.9	7840.3±776.4
Surface area of neurons in stratum moleculare (μm²)	109.4± 10.5	102.5±11.3
Surface area of neurons' nuclei in stratum moleculare (µm²)	54.5±6.3	48.2±5.7
NCR of neurons in stratum moleculare	0.325±0.033	0.216±0.039*
Number of Purkinje cells	587.4±23.1	566.6±31.5

Numerical density of Purkinje cells (mm <sup>-3</sup> )	62.1±7.7	59.2±8.9
Surface area of Purkinje cells (μm²)	542.9±66.7	461.4±60.1*
Surface area of Purkinjes' cells nuclei (µm²)	179.3±15.4	105.5±21.2*
NCR of Purkinje cells	0.355±0.037	0.312±0.033
Number of neurons in stratum granulosum	246545.7±31826.6	279856.6±30420.1
Numerical density of neurons in stratum granulosum (mm <sup>-3</sup> )	45791.8±5056.2	48023.4±5132.9
Surface area of neurons in stratum granulosum (µm²)	67.8±8.4	62.2±8.9
Surface area of neurons´ nuclei in stratum granulosum (μm²)	23.1±2.7	19.1±2.2
NCR of neurons in stratum granulosum	0.357±0.035	0.399±0.041
Number of capillary endothelial cells	167598.7±82483.3	185688.3±87251.5
Numerical density of capillary endothelial cells (μm²)	19555.5±3067.9	19111.3±7649.1
Surface area of capillary endothelial cells (μm²)	97.5±10.4	99.3±9.6

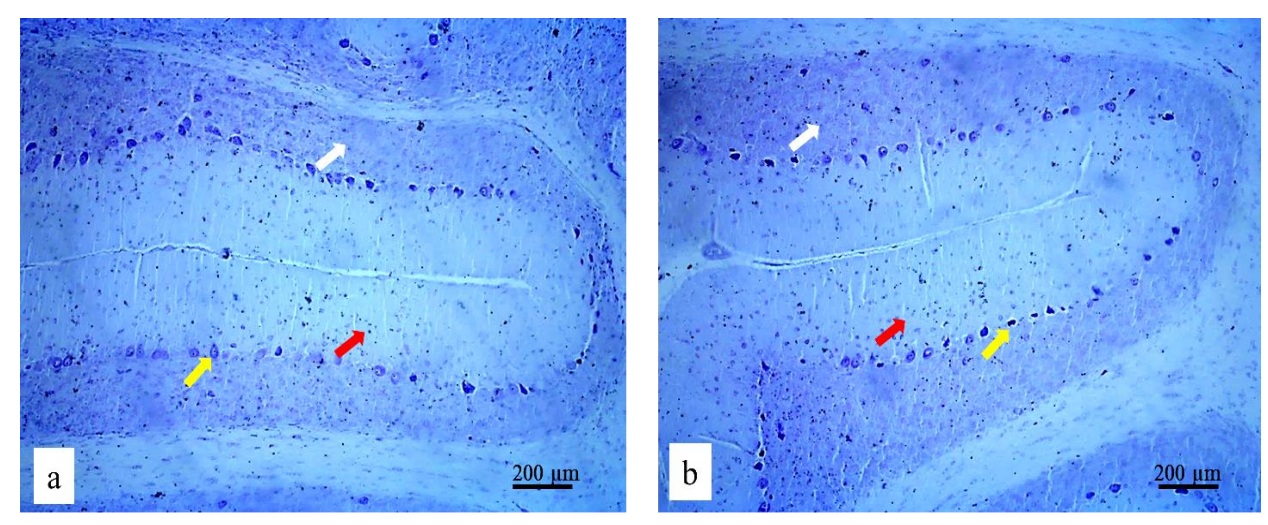


**Figure 5.** Micrographs of the histological cross-section of the rats' cerebellum, Cresyl - violet, magnification 40X. Changes in number and shape of neurons in stratum moleculare (red arrows), Purkinje cells (yellow arrows) and stratum granulosum (white arrows); control (a) and tissue treatment to Bensedin (b)

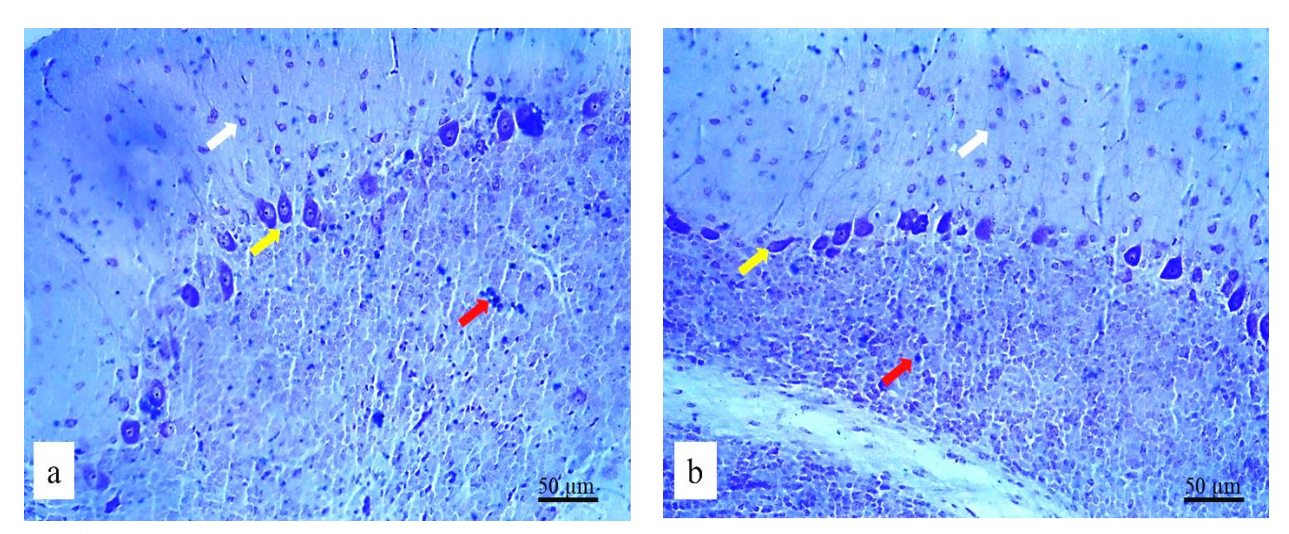


**Figure 6.** Micrographs of the histological cross-section of the rats' cerebellum, Cresyl - violet, magnification 100X. Changes in number, shape and neurite length of neurons in stratum moleculare (white arrows), Purkinje cells (yellow arrows) and stratum granulosum (red arrows); control (a) and tissue with treatment to Bensedin (b)

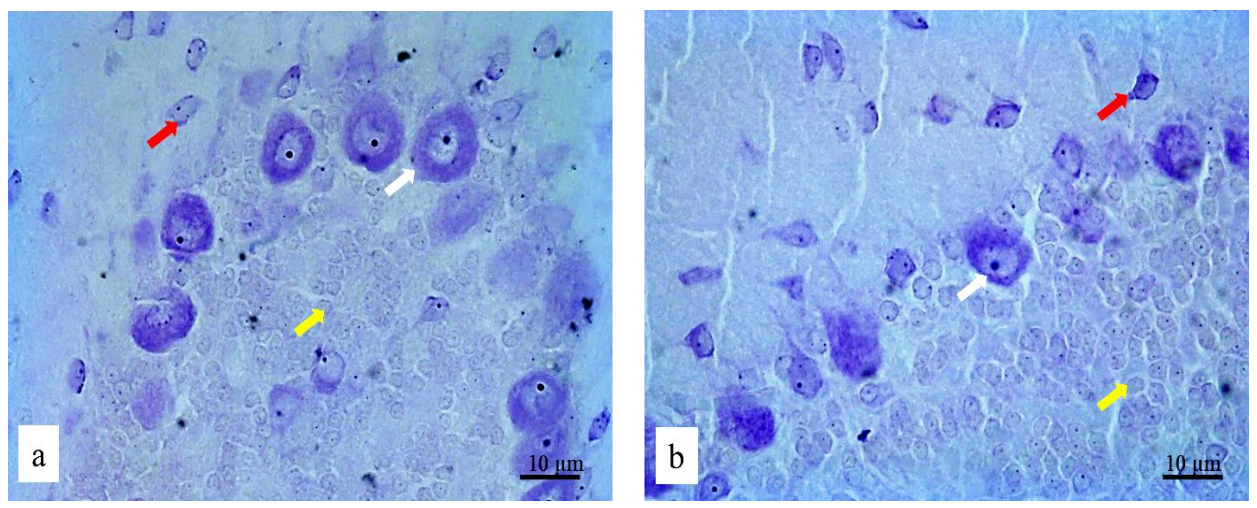


**Figure 7.** Micrographs of the histological cross-section of the rats´ cerebellum, Cresyl - violet, magnification 400X. Changes shape of Purkinje cells and their nuclei (white arrows), changes shape and numerical density of neurons in stratum moleculare (red arrows) and in stratum granulosum (yellow arrows); control (a) and tissue with treatment to Bensedin (b)

Number and numerical density of Purkinje cells and neurons in molecular layer statistically insignificantly decreased, while the same parameters in granular layer increased (Figure 5) in the Bensedin treated rat group compared to the controls (Table 2). In addition to decrease in number, there was also a change in shape of neurons in molecular and granular layers, as well as in Purkinje cells in the treated animals. A decrease in the number of neurites of Purkinje cells was also observed in the cerebella of rats treated with Bensedin (Figure 6). A statistically significant decrease in the NCR of neurons in the molecular layer (p=0.025) was noted, as well as a reduction in the surface areas of Purkinje cells (p=0.014) and their nuclei (p=0.011) in rats treated with Bensedin compared to those who were not (Figure 7). Neurons in apoptosis and mitosis were not detected in cerebellar tissue of rats even after immunohistochemical staining.

**Table 3.** Stereological parameters of the pancreas tissue of the control and experimental group of rats, value are shown as mean $\pm$ SD (\*p<0.05; t-test)

Parameters	Control	Bensedin
Volume density of endocrine pancreas (mm <sup>0</sup> )	0.108±0.014	0.162±0.021
Volume density of exocrine cells (mm <sup>0</sup> )	0.645±0.077	0.581±0.069
Volume density of connective tissue (mm <sup>0</sup> )	0.104±0.011	0.120±0.014
Volume density of capillary sinusoids (mm <sup>0</sup> )	0.112±0.014	0.134±0.022
Number of Langerhans cells	9267.3±1054.8	9895.4±1098.6
Numerical density of Langerhans cells (mm <sup>-3</sup> )	1123.7±156.5	1338.5±142.8
Surface area of Langerhans cells (μm²)	146.4±9.2	144.4±9.5
Surface area of Langerhans cells' nuclei (μm²)	65.7±6.6	66.3±6.6
NCR of Langerhans cells	0.401±0.055	0.411±0.059
Mitotic index of Langerhans cells	1.98±0.29	2.15±0.21
Number of alpha cells	21.6±3.3	66.4±8.7*
Number of acinar cells	327569.6±35616.3	277805.2±31622.2
Numerical density of acinar cells (mm <sup>-3</sup> )	40212.5±5632.9	39012.4±5534.2
Surface area of acinar cells (µm²)	139.2±11.7	144.5±12.5
Surface area of acinar cells nuclei (μm²)	44.9±6.9	45.5±7.2
NCR of acinar cells	0.384±0.042	0.359±0.041
Mitotic index of acinar cells	1.57±0.21	1.61±0.24
Number of connective tissue cells	192023.5±23463.2	258901.4±26334.9
Numerical density of connective tissue cells (mm <sup>-3</sup> )	20234.4±3486.2	22919.3±9904.5
Surface area of connective tissue cells (µm²)	88.5±9.9	86.7±9.5
Number of capillary endothelial cells	109835.2±15532.7	123936.4±18526.3
Numerical density of capillary endothelial cells (mm <sup>-3</sup> )	18582.9±2563.9	19494.2±2903.4
Surface area of capillary endothelial cells (μm²)	77.6±8.6	74.5±8.5

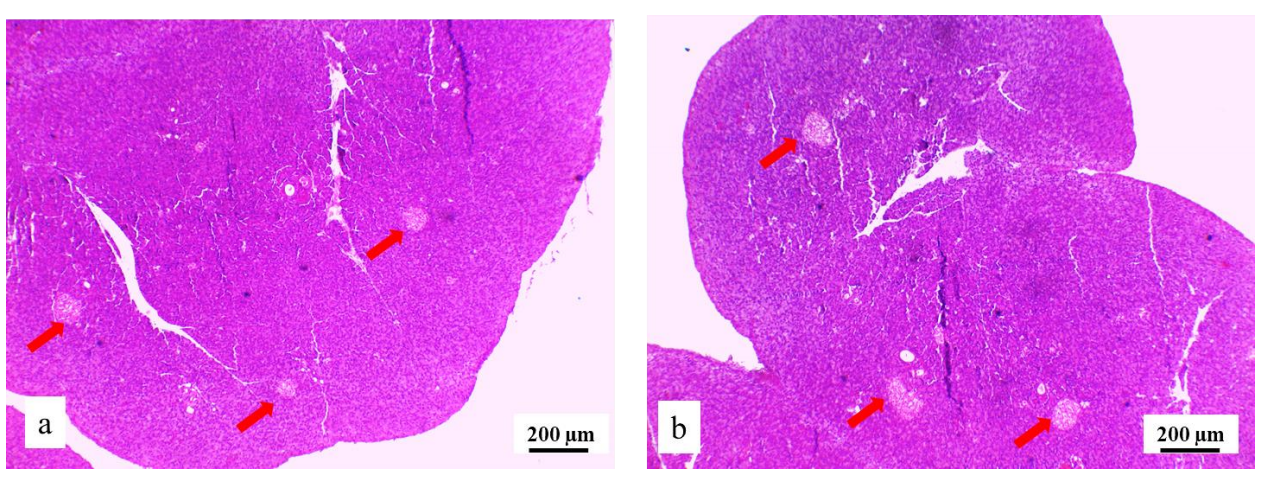


**Figure 8.** Micrographs of the histological cross-section of the rats´ pancreas, H&E, magnification 40X. Langerhans islets (red arrows); control (a) and tissue with treatment to Bensedin (b).

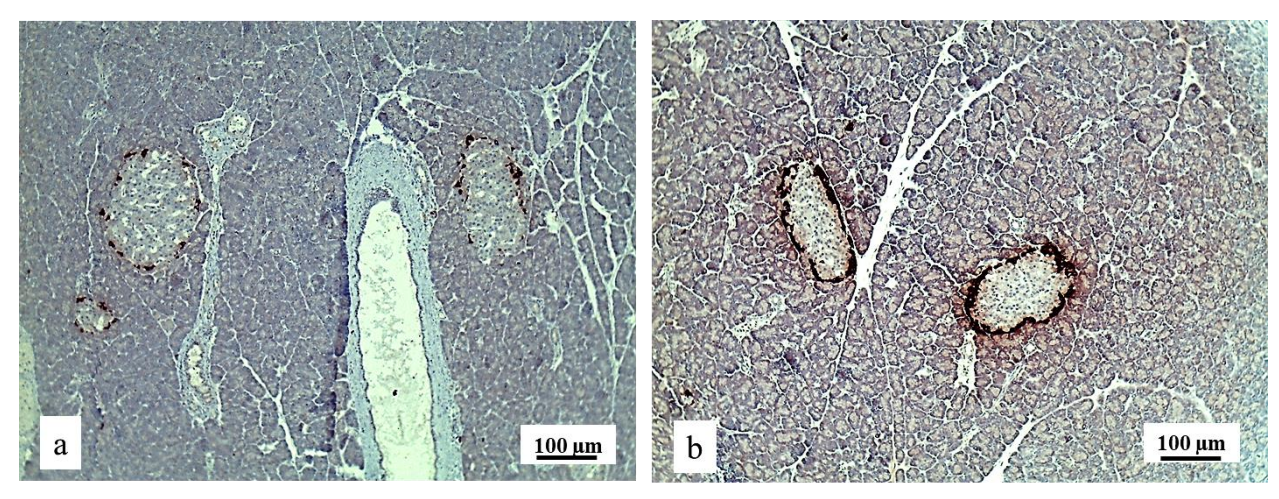


**Figure 9.** Micrographs of the histological cross-section of the rats' pancreas, Immunohistochemical glucagon-positive (alpha cells), magnification 50X. Langerhans islets; control (a) and tissue with treatment to Bensedin (b).

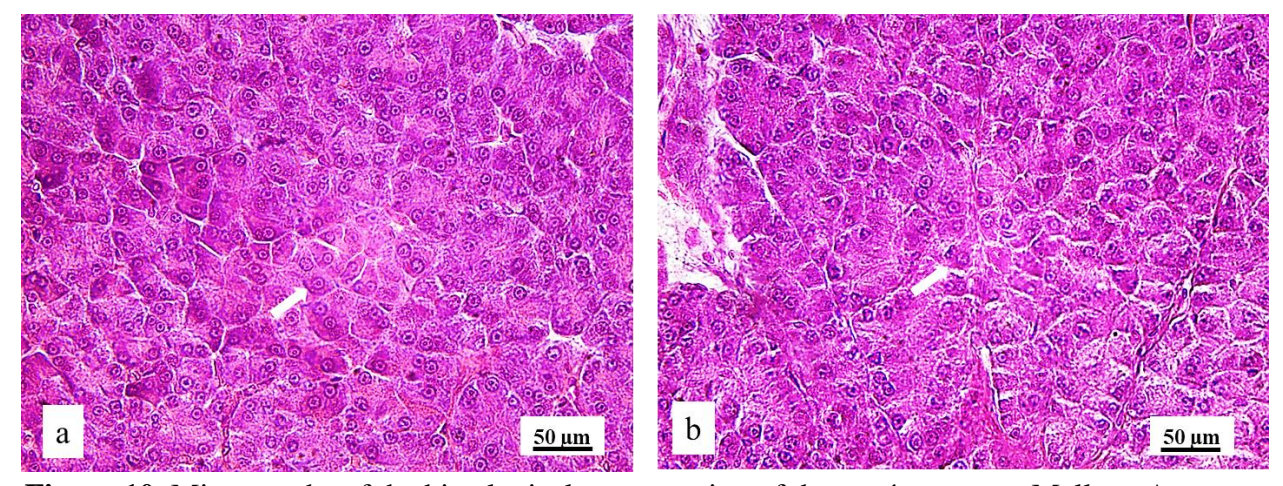


**Figure 10.** Micrographs of the histological cross-section of the rats' pancreas, Mallory-Azan, magnification 100X. Exocrine cells (white arrows); control (a) and tissue with treatment to Bensedin (b).

Values of volumetric densities of the endocrine pancreas (Figure 8), connective tissue, and sinusoidal capillaries increased in the treated rats compared to the controls. The decrease in this volumetric density is a result of the increase in the endocrine pancreas, connective tissue, and capillaries (Table 3). Immunohistochemical visualization of alpha cells in the Langerhans islets (Figure 9) shows a threefold increase in their number in the pancreases of rats treated with Bensedin compared to the controls (Table 3). This increase in number of alpha cells in the Langerhans islets was statistically significant (p=0.011) in treated rats compared to the control group. Increase in the number of alpha cells directly caused an increase in the synthesis and release of the hormone glucagon into the circulation of the treated rat group. Number and numerical density of acinar cells of the exocrine pancreas decreased, while their surface area and the surface area of their nuclei increased in treated rats with Bensedin. Exocrine pancreatic acinar cells (Figure 10) showed very little sensitivity to effect of Bensedin on their morphology. No cells in apoptosis were detected in pancreatic tissues of rats from both groups through immunohistochemical staining.

**Table 4.** Stereological parameters of the thyroid tissue of the control and experimental group of rats, value are shown as mean±SD (\*p<0.05; t-test)

Parameters	Control	Bensedin
Volume density of thyrocytes (mm <sup>0</sup> )	0.341±0.051	0.320±0.055
Volume density of capillary sinusoids (mm <sup>0</sup> )	0.211±0.023	0.248±0.037
Volume density of connective tissue (mm <sup>0</sup> )	0.167±0.011	0.198±0.014
Volume density of colloid (mm <sup>0</sup> )	0.295±0.031	0.218±0.029*
Number of thyrocytes	125357.6±11252.5	101859.1±10495.2
Numerical density of thyrocytes (mm <sup>-3</sup> )	20794.3±2534.7	16357.9±2295.1
Surface area of thyrocytes (μm <sup>2</sup> )	128.5±15.5	207.7±18.4*
Surface area of thyrocytes nuclei (µm²)	66.5±9.9	69.8±8.9
NCR of thyrocytes	0.243±0.025	0.310±0.029*
Mitotic index of thyrocytes	1.65±0.13	1.55±0.11
Number of connective tissue cells	84836.4±10467.3	131553.2±11252.7
Numerical density of connective tissue cells (mm <sup>-3</sup> )	9153.6±8675.1	11095.8±9904.5
Surface area of connective tissue cells (µm²)	97.4±10.2	99.6±10.9
Number of capillary endothelial cells	111455.7±15573.6	139364.6±17909.5
Numerical density of capillary endothelial cells (mm <sup>-3</sup> )	10858.4±1366.1	12043.2±1472.1
Surface area of capillary endothelial cells (μm²)	84.4±11.5	89.6±12.1

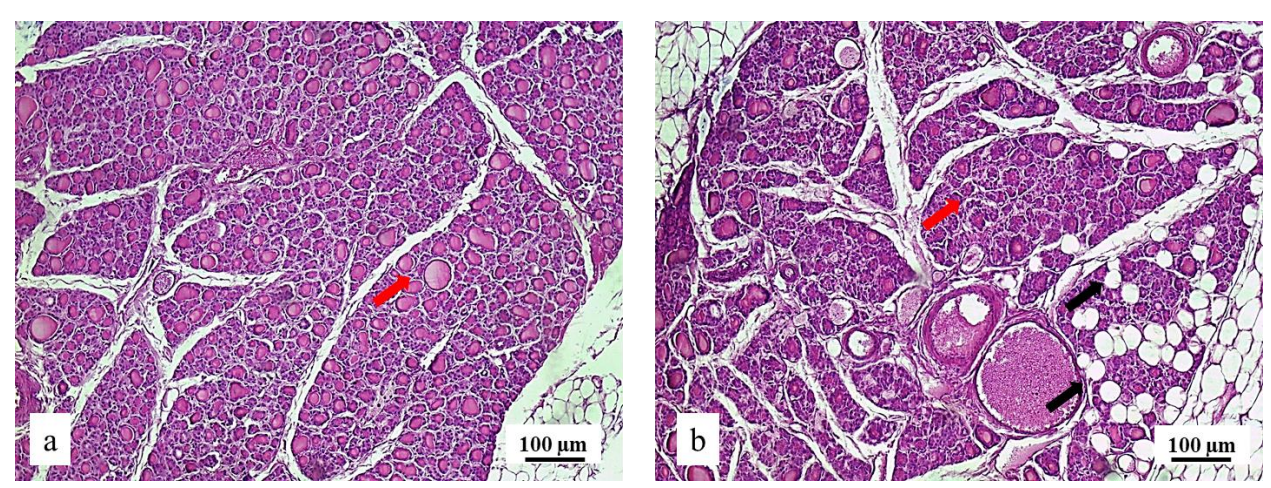


**Figure 11.** Micrographs of the histological cross-section of the rats' thyroid gland, H&E, magnification 50X. Follicles (red arrows), thyreocytes and microcavities (black arrows); control (a) and tissue treatment to Bensedin (b).

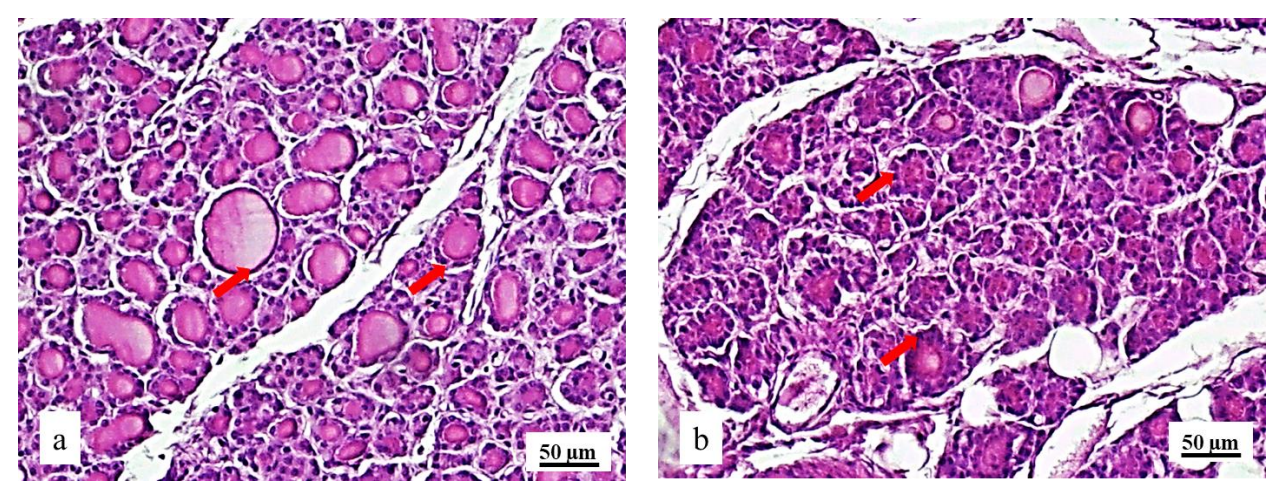


**Figure 12.** Micrographs of the histological cross-section of the rats' thyroid gland, H&E, magnification 100X. Thyreocytes (red arrows) and connective tissue; control (a) and tissue with treatment to Bensedin (b)

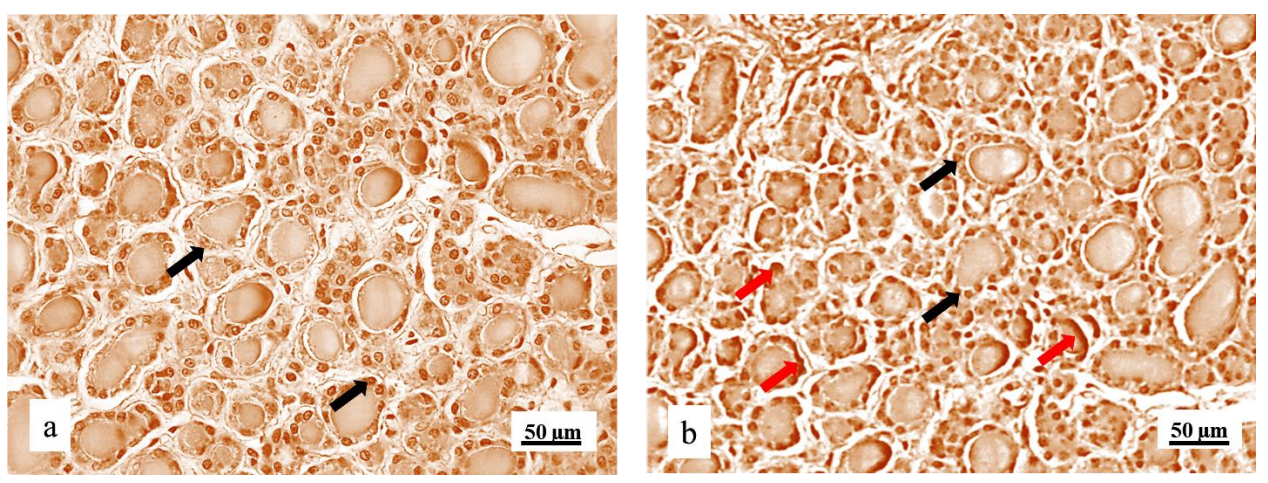


**Figure 13.** Micrographs of the histological cross-section of the rats' thyroid gland, BLX-CX, magnification 100X. Thyreocytes (black arrows) and thyreocytes with high immunereactions (red arrows); control (a) and tissue with treatment to Bensedin (b)

Largest changes in the thyroid gland tissues occurred in the reduction of the volumetric density values of the colloid in the follicles (Table 4), which was statistically significant (p=0.034). In addition to this decrease, empty follicles and microcavities, areas without follicles in the thyroid tissue of the treated rat group, appeared (Figure 11). Volumetric densities of sinusoidal capillaries and connective tissue increased, while those of thyrocytes decreased in the Bensedin treated rats (Table 4). Number and numerical density of thyrocytes in the thyroid gland tissues of rats treated with Bensedin decreased, but their surface area statistically significantly (p=0.019) increased compared to the control rats (Figure 12). The NCR of thyrocytes statistically significantly increased (p=0.041) due to changes in the volume of thyrocytes, while the volume of their nuclei remained unchanged in the treated animals compared to the controls. In line with the increased volumetric densities of connective tissue and sinusoidal capillaries, the values of the number and numerical density of the cells forming connective tissue and blood vessels in the thyroid glands of treated rats increased. Volumetric density, number, and numerical density of connective tissue increased due to the appearance of microcavities in the thyroid tissue of the treated rat group. Immunohistochemical analysis of thyroid gland tissue did not detect thyrocytes in apoptosis, but a stronger immunoreaction of surviving (Figure 13) was observed in the thyrocytes of the thyroid glands of rats treated with Bensedin.

## **DISCUSSION**

This paper is a continuation of the presentation of results from the same study, which demonstrated changes in the cytoarchitecture of liver, kidney, and spleen tissues in rats following oral administration of Bensedin (Grahovac et al., 2019). Diazepam, as a longacting benzodiazepine, reduces microglial activity, preventing them from effectively protecting the rat brain from neurological changes (Griffin et al., 2013). Negative effects were shown in our work as well. Numerous literature sources confirm that diazepam has harmful effects on nervous tissues, particularly on nerve cells and nerve fibers, as it increases oxidative processes and leads to their apoptosis (Badawy et al., 2014; Mousa et al., 2014). Presence of neuron apoptosis was demonstrated by histological analysis in our work as well. Diazepam induces an imbalance of ions in the rat body, which further causes dysfunction of nervous tissue, altered heart function, and muscle contractility (Stevens et al., 2017). The cessation of diazepam's effects results in electrolyte imbalance, which alters signaling, structural, metabolic, and regulatory proteins on the membranes of nerve and muscle cells (Al-Abbasi et al., 2020). Following diazepam administration, the enzymatic activity of neurons, which constitute every organ in the rat's body, is entirely altered (Amin et al., 2019). Diazepam reduces the activity of glutathione reductase in all nerve fibers and diminishes the self-protective role of microglia and neurons (Supasai et al., 2020). Changes in cytoarchitecture of the cerebellum and the cerebrum in rats treated with diazepam in our work show a change in the enzymatic activity of the neurons that build them. Upon discontinuation of diazepam, hyperactivity of the pancreas and the thyroid gland occurs due to increased mobilization of cholesterol from hepatocytes into the bloodstream (Ilesanmi et al., 2020; Joyce et al., 2018). Long-term use of diazepam can lead to histopathological disorders in the tissues of the cerebrum and the cerebellum, as well as the pancreas and the thyroid gland in

rats (Osonuga et al., 2012). Diazepam induces inflammatory processes, vascular congestion, sinusoidal dilation, and vacuolar degeneration in brain, pancreatic, and thyroid tissues (Hurst et al., 2017). Diazepam affects the immune system by reducing the number of inflammatory and infiltrating immune cells in the central nervous system of mice during the acute phase of experimental autoimmune encephalomyelitis. Reduction in immune response cells leads to a decrease in the number of inflammatory cells, like microglia, monocytes and macrophages in pancreas, thyroid and brain tissues of rats exposed to benzodiazepine treatment (Mohamed et al., 2020). Reduction cells of immune system and elements of cardiovascular system after use of diazepine in our experiment negatively affects work of pancreas, thyroid gland and nervous tissue. These claims are confirmed by stereological parameters. Diazepam disrupts the proper functioning of the pancreas, and its long-term use causes changes in the morphology of insulin-producing cells (Abed et al., 2013). Sedation of the endocrine system by diazepam affects the reduction in cell size within the pancreas and their nucleocytoplasmic ratio (Sayed et al., 2011). This result was also obtained in our experiment. Diazepam alters the cytoarchitecture of thyroid tissue in rats by causing an expansion in colloid volume and a reduction in thyrocyte height, as also reported in the literature (Ali et al., 2014). Morphological changes in the thyroid gland caused by sedative drugs are reversible if not administered over extended periods (De et al., 2012).

## **CONCLUSIONS**

Rapid and effective sedative effect of diazepam on neurons of the cerebrum and the cerebellum, as well as the cells of the pancreas and the thyroid gland, is primary reason for its widespread therapeutic use in both humans and animals. In this study, a fifteen-day oral treatment with diazepam affected histological and stereological parameters in tissues of cerebrum, cerebellum, pancreas and thyroid gland of rats treated with Bensedin. Changes were observed in cytoarchitecture of all cells that make up the organs examined in this study. Therefore, dosage and duration of diazepam therapy must be individually adjusted.

## **ACKNOWLEDGMENTS**

Authors thank the Ministry of Scientific and Research Development, Higher Education and Information Society of Republic of Srpska for the projects support (Contract numbers: 19/6-20/961-98/18 and 19/6-20/961-66/18).

#### REFERENCES

- Abed, A., Minaiyan, M., Safaei, A. & Taheri, D. (2013). Effect of diazepam on severity of acute pancreatitis: possible involvement of peripheral benzodiazepine receptors. *ISRN Gastroenterology*, 2013:484128. <a href="https://doi.org/10.1155/2013/484128">https://doi.org/10.1155/2013/484128</a>
- Al-Abbasi, F., Kumar, V. & Anwar, F. (2020). Biochemical and toxicological effect of diazepam in stress-induced cardiac dysfunctions. *Toxicology Reports*, 7, 788-794. <a href="https://doi.org/10.1016/j.toxrep.2020.06.004">https://doi.org/10.1016/j.toxrep.2020.06.004</a>

- Aleksandrov, A., Šegrt, Z., Jaćević, V., Kilibarda, V. & Potrebić, O. (1999). Farmakodinamski i farmakokinetski efekti primene flumazenila i teofilina kod pacova akutno trovanih diazepamom. *Vojnosanitetski Pregled*, 66(2), 141-148.
- Ali, A., Zinad, K. & Karhan, H. (2014). Histopathological changes and immunosuppression induce by diazepam in mice. *Al-Qadisiyah Journal of Veterinary and Medicine Sciences*, 13(1), 59-65. https://doi.org/10.29079/VOL13ISS1ART279
- Amin, M., Khanam, S., Mazumder, L., Rahman, Z., Anower, M. & Mollah, M. (2019). Evaluation of some prescribed and over-the-counter drugs induced hemato-biochemical changes in mice. *Asian Journal of Medical and Biological Research*, 5(4), 297-302. https://doi.org/10.3329/ajmbr.v5i4.45268
- Amorim, C. G., Araújo, A. N., Montenegro, M. C. & Silva, V. L. (2008). Cyclodextrin-based potentiometric sensors for midazolam and diazepam. *Jornal of Pharmaceutical and Biomedical Analysis*, 48(3), 1064-1069. https://doi.org/10.1016/j.jpba.2008.08.012
- Anber, Z., Fadhil, A. & Anber, S. (2018). The biochemical and histological effect of diazepam on the liver of albino male rats. *International Journal of Academic Research and Reflection*, 6(3), 8-16.
- Ashton, H. (2005). The diagnosis and management of benzodiazepine dependence. *Current Opinion ih Psychiatry*, 18(6), 249-255. doi: 10.21608/ajfm.2014.18756
- Badawy, S., Hammad, S., Amin, S., Zanaty, A., Mohamed, R. & Aid, H. (2014). Effects of Dependence of Tramadol, Diazepam and Their Combination on the Brain of Albino Rats: Biochemical, Histological and Immunohistochemical Study. *Ain Shams Journal of Forensic Medicine and Clinical Toxicology*, 23(2), 139-147. doi: 10.21608/ajfm.2014.18756
- De, P., Pang, T. & Das, G. (2012). Clinical Implications and Management of Sub Clinical Hyperthyroidism: A Review. *Open Journal of Endocrine and Metabolic Diseases*, 2(3), 27-35. doi: 10.4236/ojemd.2012.23004
- Eman, A., Al-Rekabi, S. & Zalar, A. R. (2021). Effect of tramadol and diazepam on some biochemical parameters of male rats. *Journal of Natural Remedies*, *14*(2), 303-319.
- Grahovac, J., Ivanović, M., Dekić, R. & Paraš, S. (2019). Effects of diazepam on hematological and histological parameters in rats / in vivo and unbiased stereological investigation. *Acta Veterinaria Beograd*, 72(2), 235-255. https://doi.org/10.2478/acve-2022-0019
- Griffin, E., Kaye, M., Bueno, R. & Kaye, D. (2013). Benzodiazepine Pharmacology and Central Nervous System–Mediated Effects. *Ochsner Journl*, *13*(2), 214-223. PMID: 23789008; PMCID: PMC3684331.
- Honeychurch, K. C., Hart, J. & Peree, M. (2014). Electrochemical Detection of Benzodiazepines, Following Liquid Chromatography, for Applications in Pharmaceutical, Biomedical and Forensic Investigations. *Insciences Jornual*, *3*(24), 1-18. doi:10.5640/insc.040101
- Hurst, N., Zanetti S., Baez, N, Bibolini, C. & Roth, G. (2017). Diazepam treatment reduces inflammatory cells and mediators in the central nervous system of rats with experimental autoimmune encephalomyelitis. *Journal of Neuroimmunology*, *15*(313), 145-151. DOI: 10.1016/j.jneuroim.2017.09.012

- Ilesanmi, O. B., Odewale, T. & Tomas, Y. (2020). Effect of classic soft drink Coca-Cola as a solvent in the administration of tramadol and diazepam on biochemical and histological changes in liver and kidney. *Ukrainian Journal of Nephrology and Dialysis*, 4(2), 33-41. https://doi.org/10.31450/ukrjnd.3(67).2020.06
- Joyce, N., Augustin, U. & Onuoha, S. (2018). Impact of benzodiazepines administration on selected biochemical parameters of albino Wistar rats (*Rattus rattus*). *Egyptian Pharmaceutical Journal*, 17(1), 1-40. DOI: 10.4103/epj.epj\_26\_17
- Malcolm, R. J. (2003). GABA Systems, Benzodiazepines, and Substance Dependence. *Journal of Clinical Psychiatry*, 64(3), 36-40. PMID: 12662132
- Mimica, N., Folnegović-Šmalc, V., Uzun, S. & Rušinović, M. (2002). Benzodiazepini: za i protiv. *Medicus*, 11(2), 183-188.
- Mohamed, A., Hosney, M., Bassiony, H., Hassenein, S., Soliman, A., Fahmy, S. & Gaafar, K. (2020). Sodium pentobarbital dosages for exsanguination affect biochemical, molecular and histological measurements in rats. *Scientific Reports*, 10, 378. <a href="https://doi.org/10.1038/s41598-019-57252-7">https://doi.org/10.1038/s41598-019-57252-7</a>
- Mousa, A., Amany, M. & Hassiony, V. (2014). Light and electron microscopic study on the effect of diazepam on the cardiac muscle of adult albino rat and the possible role of garlic. *The Egyptan Journal of Histology*, *37*(1), 102-111. DOI: 10.1097/01.EHX.0000444077. 09624.b1
- Nestorović, M., Trifunović, S., Jarić, I., Manojlović-Stojanoski M., Ristić, N., Filipović, B., Šošić-Jurević, B. & Milošević, V. (2016). Sex steroid application reverses changes in rat castration cells: Unbiased stereological analysis. *Archives of Biological Sciences*, 68(4), 821-828. <a href="https://doi.org/10.2298/ABS151201070N">https://doi.org/10.2298/ABS151201070N</a>
- Olfson, M., King, M. & Schoenbaum, M. (2015). Benzodiazepine Use in the United States. *JAMA Psychiatry*, 72(2), 136–142. doi:10.1001/jamapsychiatry.2014.1763
- Osonuga, I., Osonuga, O., Osonuga, A., Onadeko, A. & Osonuga, A. (2012). Effect of artemether on hematological parameters of healthy and uninfected adult Wistar rats. *Asian Pacific Journal of Tropical Biomedicine*, 2(6), 493-495. https://doi.org/10.1016/S2221-1691(12)60083-5
- Owen, G., Smith, T. H. & Agersborg, H. P. (1970). Toxicity of some benzodiazepine compounds with CNS activity. *Toxicoloxy and Applied Pharmacology*, *16*(2), 556-570. https://doi.org/10.1016/0041-008X(70)90031-1
- Paraš, S., Janković, O., Trišić, D., Čolović, B., Mitrović-Ajtić, O., Dekić, R., Soldatović, I., Živković-Sandić, M., Živković, S. & Jokanović, V. (2019). Influence of nanostructured calcium aluminate and calcium silicate on the liver: histological and unbiased stereological analysis. *International Endodontic Jornal*, *52*(8), 1162-1172. <a href="https://doi.org/10.1111/iej.13105">https://doi.org/10.1111/iej.13105</a>
- Pomares, F. B., Funck, T., Feier, N., Roy, S., Ceko, M. & Narayanan, S. (2017). Histological Underpinnings of Grey Matter Changes in Fibromyalgia Investigated Using Multimodal Brain Imaging. *The Journal of neuroscience: the official journal of the Society for Neuroscience, 37*(5) 1090-1101. <a href="https://doi.org/10.1523/JNEUROSCI.2619-16.2016">https://doi.org/10.1523/JNEUROSCI.2619-16.2016</a>
- Sayed, G., Desoky, N., El-Refaiy, A., Abd-Elrahman, I. & Nagy, M. (2011). Histological study on the stomach of immobilized-stressed albino rat and the curative role of diazepam. *Egyptian Journal of Experimental Biology Zoology*, 7(2), 153-161.

- Setiawan, P., Tunjung, W. & Nurhidayat, L. (2016). Effect of diazepam on kidney function and histological structure of white rats. *Journal of Biological Research*, 22(1), 1-6. DOI:10.23869/bphjbr.22.1.20161
- Sevastre-Berghian, A. C., Fagarasan, V., Toma, A. V., Baldea, I., Olteanu, D. & Moldovan, R. (2017). Curcumin Reverses the Diazepam-Induced Cognitive Impairment by Modulation of Oxidative Stress and ERK 1/2/NF-κ B Pathway in Brain. *Oxidative Medicine and Cellular Longevity*, 2017:3037876. https://doi.org/10.1155/2017/3037876
- Stevens, C., Rayani, K., Singh, G., Lotfalisalmasi., B., Tieleman, P. & Tibbits, G. (2017). Changes in the dynamics of the cardiac troponin C molecule explain the effects of Ca2+-sensitizing mutations. *Journal of Biological Chemistry*, 292(28), 11915-11926. <a href="https://doi.org/10.1074/jbc.M116.770776">https://doi.org/10.1074/jbc.M116.770776</a>
- Supasai, S., Gonzalez, E., Rowland, D., Hobson, B., Bruun, D., Guignet, M., Soeres, S., Singh, V., Wulff, H., Saito, N., Harvey, D. & Lein, P. (2020). Acute administration of diazepam or midazolam minimally alters long-term neuropathological effects in the rat brain following acute intoxication with diisopropylfluorophosphate. *European Journal of Pharmaceutical Sciences*, 886:173538. <a href="https://doi.org/10.1016/j.ejphar.2020.173538">https://doi.org/10.1016/j.ejphar.2020.173538</a>

# ЕФЕКТИ ДИАЗЕПАМА НА ХИСТОЛОШКЕ ПРОМЕНЕ ТКИВА ВЕЛИКОГ И МАЛОГ МОЗГА, ПАНКРЕАСА И ШТИТНЕ ЖЛЕЗДЕ ПАЦОВА

Јована Граховац $^1$ , Миленка Ивановић $^1$ , Радослав Декић $^{\dagger}^1$ , Маја Шибаревић $^1$ , Смиљана Параш $^{1*}$ 

<sup>1</sup>Универзитет у Бањој Луци, Природно-математички факултет, Младена Стојановића 2, 78000 Бања Лука, Република Српска, Босна и Херцеговина \*Кореспондентни аутор: smiljana.paras@pmf.unibl.org

#### Сажетак

Диазепам је лек који се данас широко користи за лечење људи, као примарни лек код лечења неуролошких поремећаја или као помоћна терапија за симптоматско лечење других обољења. Диазепам изазива опуштајући ефекат организма као резултат седативног деловања на централни нервни систем. Својим директним утицајем на нервни систем, диазепам ремети правилно функционисање свих органа у људском телу. Циљ овог рада био је да прошири досадашња истраживања о утицају диазепама на хистолошке параметре великог и малог мозга, панкреаса и штитне жлезде код пацова. Дизајн експеримента је укључивао две групе експерименталних животиња, од којих је једна третирана диазепамом, а друга није. У студији су кориштене методе хистолошких бојења ткива пацова: хемтоксилин-еозин, Mallory-Azan и имуно-хистохемијске методе бојења (ВLX-СХ и сурвивин). Цитометријском анализом детектоване су ћелије које у апоптози, а мерења стереолошких параметара вршена су

коришћењем стереолошког универзалног тест система заснованог на Кавалијеријевом принципу. Резултати хистолошке и стереолошке анализе параметара указују на промене у цитоархитектури ткива великог и малог мозга, панкреаса и штитне жлезде код пацова изложених диазепаму у односу на оне који нису били изложени. Промене у хистолошким параметрима анализираних ткива органа пацова директно показују да диазепам утиче на њихову правилну функцију. Ова студија пружа основу за даља детаљна научна истраживања која имају за циљ да разјасне постојеће ефекте диазепама на све органе у организму пацова.

Кључне речи: диазепам, велики и мали мозак, панкреас, штитна жлезда

Received February 15, 2025 Accepted June 25, 2025